JACS
JOURNAL OF THE AMERICAN CHEMICAL SOCIETY
Communication
pubs.acs.org/JACS

# Dynamics of a Globular Protein Adsorbed to Liposomal Nanoparticles

Alberto Ceccon,[†] Moreno Lelli,[‡] Mariapina D'Onofrio,[†] Henriette Molinari,[⊥] and Michael Assfalg*[,†]

[†]Department of Biotechnology, University of Verona, Strada Le Grazie 15, 37134 Verona, Italy

[‡]Centre de RMN à Trés Hauts Champs, Institut de Sciences Analytiques, Université de Lyon, CNRS/ENS Lyon/UCB Lyon 1, 69100 Villeurbanne, France

[⊥]Laboratorio NMR, Istituto per lo Studio delle Macromolecole, CNR, Via Bassini 15, 20133 Milano, Italy

Supporting Information

**ABSTRACT:** A solution-state NMR method is proposed to investigate the dynamics of proteins that undergo reversible association with nanoparticles (NPs). We applied the recently developed dark-state exchange saturation transfer experiment to obtain residue-level dynamic information on a NP-adsorbed protein in the form of transverse spin relaxation rates, $R_2^{bound}$. Based on dynamic light scattering, fluorescence, circular dichroism, and NMR spectroscopy data, we show that the test protein, human liver fatty acid binding protein, interacts reversibly and peripherally with liposomal NPs without experiencing significant structural changes. The significant but modest saturation transfer from the bound state observed at 14.1 and 23.5 T static magnetic fields, and the small determined $R_2^{bound}$ values were consistent with a largely unrestricted global motion at the lipid surface. Amino acid residues displaying faster spin relaxation mapped to a region that could represent the epitope of interaction with an extended phospholipid chain constituting the protein anchor. These results prove that atomic-resolution protein dynamics is accessible even after association with NPs, supporting the use of saturation transfer methods as powerful tools in bionanoscience.

Protein–nanoparticle interactions have a dramatic impact in the fields of nanobiology, nanomedicine, and all related scientific areas.[1−3] For example, it has been recognized that upon exposure to a biological medium, nanoparticles (NPs) adsorb a variety of biomolecules, forming a complex dynamic layer (protein corona).[4] Protein–NP interactions are also of interest for the development of hybrid devices,[5] and NPs can influence protein self-assembly reactions,[6] sometimes posing toxicity issues.[7,8] Translocation of a protein from bulk solution to the NP surface represents a major change in the protein's environment which may lead to profound perturbations of chemical properties and biological activity.[9] Thus, methodologies aimed at characterizing biomolecules bound to NPs represent an indispensable tool in bionanoscience.[10]

Protein conformational changes induced by association with NPs have been detected by several spectroscopic techniques.[11] Time-averaged protein structures often provide enough information to understand their functions; however, it is recognized that biomacromolecules are complex dynamic systems, whose flexibility reflects important mechanistic aspects of function.[12−14] It can be predicted that NPs will profoundly reshape the protein conformational energy landscape and modify motional amplitudes and time scales. However, this aspect has received little consideration in experimental assays, and computational approaches have been used instead.[15,16] Solution-state nuclear magnetic resonance (NMR) spectroscopy is a prominent technique in biomolecular dynamics investigations.[17] Protein dynamics can be derived from the measurement of spin relaxation rates, which are influenced by both global macromolecular tumbling and internal motion.[17] Large supramolecular adducts are characterized by slow rotational diffusion which causes very fast transverse spin relaxation and, ultimately, extremely broad or even undetectable signals. On these premises, direct investigation of molecular motion for proteins adsorbed to even medium-sized NPs is difficult with standard NMR experiments.

Reversible binding equilibria offer an opportunity to circumvent the intrinsic size-limitation of high resolution NMR. Recently, a novel method, the dark-state exchange saturation transfer experiment (DEST),[18] has been developed to characterize the atomic-level dynamics of unstructured polypeptides transiently bound to large polymorphic aggregates[18b] or to huge molecular chaperone proteins.[18d] In the DEST experiment, the $^{15}$N magnetization of the observable species is transferred by chemical exchange to the corresponding invisible state, partly saturated (perturbed), and transferred back upon dissociation from the high-molecular-weight species. The large transverse relaxation rates ($R_2$) of the supramolecular entity preclude direct observation but allow for efficient partial saturation of the magnetization by a weak radio frequency field, even at large offsets where the signals of the visible species are unaffected. Partial saturation is recorded as an attenuation of the signals of the visible species. The combination of DEST and two-dimensional $^1$H,$^{15}$N-heteronuclear correlation allows to obtain single-residue resolution dynamic information on the NMR-invisible state in the form of $^{15}$N-$R_2$ values.[18c] Exchange processes accessible by DEST occur on time scales ranging from ∼0.01 to ∼1 s.

In this work we wished to investigate whether the DEST approach could be exploited to measure atomic-level dynamics

**Received:** July 18, 2014
**Published:** September 8, 2014

   dx.doi.org/10.1021/ja507310m | J. Am. Chem. Soc. 2014, 136, 13158−13161

of proteins interacting with liposomes. The influence of soft NPs, such as liposomes, on protein chemistry has received little attention compared to that of "hard" nanomaterials.[19] Liposomes are spherical vesicles consisting of single or multiple concentric lipid bilayers encapsulating an aqueous compartment. The success of liposomes is related to their role as drug nanocarriers.[20] We sought for test proteins considered able to associate with liposomes and chose the human liver fatty acid binding protein (LFABP), a ∼15 kDa globular polypeptide playing a key role in intracellular lipid trafficking.[21] Proteins of the FABP family are water-soluble but they were also shown to display membranotropic behavior, being transiently recruited to cell membranes.[22,23] Human LFABP in its unbound form is best described by an ensemble of conformational states in equilibrium and its fluctuations were proposed to be functional for molecular recognition.[24,25] The dynamic nature of LFABP makes it an appropriate choice to study NP-induced changes in local mobility. Based on the capability of LFABP to interact with lipid membranes, we investigated the dynamic association equilibrium with pristine lipid NPs. The latter were prepared as large unilamellar vesicles composed of palmitoyl-oleoyl-phosphatidylglycerol (POPG) and/or -phosphatidylcholine (POPC) and cholesterol (Chl) in different proportions. Analysis by dynamic light scattering (DLS) yielded an average diameter of ∼90 nm and a polydispersity index of ∼0.05.

Experimental evidence was accumulated to demonstrate the occurrence of LFABP−NP interactions in different conditions. On addition of LFABP, an increase in the hydrodynamic size of POPC:POPG(1:1)−NPs was clearly detected by DLS (Figure 1a), together with a decrease of the zeta-potential (Supporting

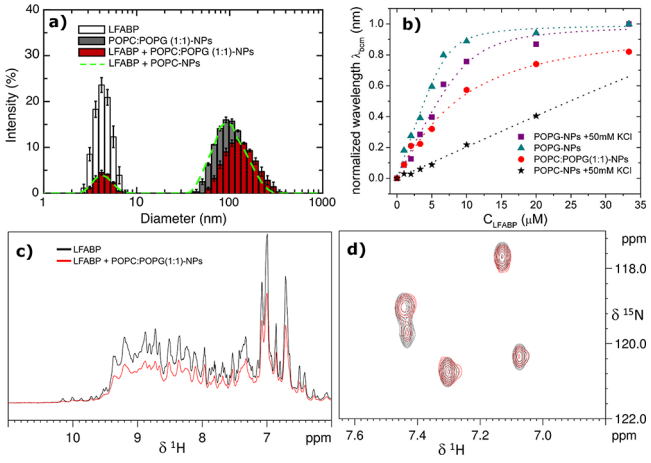


**Figure 1.** Monitoring LFABP binding to liposomal NPs. (a) DLS-derived size distribution of LFABP, NPs, and protein:NP mixtures. (b) Fluorimetric titration plots reporting the variation of the barycentric mean fluorescence of NPs incorporating the fluorescent lipid dansyl-DHPE, on addition of LFABP to 10 $\mu$M lipid. (c) Downfield portion of 1D $^{1}$H NMR spectra of LFABP alone and after addition of NPs. (d) Portion of overlaid $^{1}$H,$^{15}$N-HSQC NMR spectra of LFABP alone and in the presence of NPs. Protein:lipid molar ratios were 1:40.

Information (SI), Figure S1). Addition of LFABP to NPs incorporating 10% mol/mol of the fluorescent lipid dansyl-DHPE resulted in enhanced fluorescence emission and a blue-shift of the maximum emission wavelength, consistent with a decreased polarity of the environment around the fluorophore in the context of the NP−protein interface compared to the NP−solvent interface. The fluorimetric titration data showed a hyperbolic dependence of the fluorescence emission on protein concentration (Figure 1b), suggestive of a reversible two-state binding equilibrium. Additional evidence of the reversibility of the process was obtained from steady-state and real-time fluorescence measurements (Figure S2 and SI for details). From analysis of the binding isotherms corresponding to different lipid compositions and/or salt concentrations, it was found that binding affinity decreased in the order POPG−NP > POPG−NP + 50 mM KCl > POPG:POPC−NP > POPC−NP + 50 mM KCl, clearly indicating that electrostatic attractions contributed substantially to the association. The 1D $^{1}$H NMR spectra of LFABP in the presence of NPs (Figure 1c) reflected the same trends observed by fluorimetry. The signals in the downfield region, displaying no lipid resonances, exhibited strong intensity attenuation in the presence of POPG−NPs at low ionic strength, a moderate attenuation with POPG−NPs at higher ionic strength, and no perturbation with POPC−NPs. The 2D $^{1}$H,$^{15}$N heteronuclear single quantum coherence (HSQC) spectra recorded on $^{15}$N-labeled LFABP in the presence of NPs displayed analogous intensity changes and only minor position changes of the resonances (Figure 1d), indicating unperturbed chemical environments of individual amide groups of the free protein. By comparison of circular dichroism spectra of LFABP recorded in the absence and in the presence of POPG−NPs we assessed the integrity of the structure in the bound state (Figure S3). Dissociation rates were determined from fluorescence intensity decays, displaying monoexponential trends with rate constants $k_{off}$ = 0.71 ± 0.13 $s^{-1}$ (POPC:POPG−NP) and $k_{off}$ = 0.014 ± 0.002 $s^{-1}$ (POPG−NP), confirming the more rapid dissociation from NPs bearing lower global negative charge.

The above analysis allowed us to identify the key factors that modulate the binding affinities and exchange rates for the investigated protein−NP system. We screened the conditions for obtaining the largest DEST effect using a quick 1D implementation of the $^{15}$N-DEST experiment. A small but significant and reproducible DEST effect (larger attenuation profile) was detected for a sample constituted by LFABP and POPC:POPG−NPs at a protein:lipid molar ratio of 1:40, dissolved in phosphate buffer containing 50 mM KCl (Figure 2a). The observed effect reflected saturation produced on the NMR-invisible protein−NP adduct transferred to free LFABP signals by chemical exchange. Several other sample preparations resulted in unperturbed saturation profiles possibly due to unfavorable binding affinities, population fractions, or dissociation rates. The 2D $^{15}$N-DEST experiment was then performed on the favorable sample as well as on control samples containing the protein alone or in the presence of POPG−NPs or POPC−NPs. In this case, the DEST effect could be evaluated on a residue-level and selected saturation profiles measured at 23.5 T (1000 MHz of $^{1}$H Larmor frequency) are shown in Figure 2b−d. An important observation at this stage was that DEST was not equal for all residues, as expected for a rigid globular macromolecule, but varied along the protein chain, reflecting local dynamics (residue-specific $^{15}$N-$R_2$) of LFABP in the NP-bound state.

Observation of a DEST effect implies that a difference in protein $R_2$ values should be observed upon addition of NPs, even in the absence of major chemical shift perturbations. Indeed, $^{15}$N-$R_2$ values measured on LFABP in the presence of POPC:POPG−NPs (and 50 mM KCl) were generally larger than the corresponding values measured for the protein alone or those determined for LFABP in the presence of POPC−


dx.doi.org/10.1021/ja507310m | J. Am. Chem. Soc. 2014, 136, 13158−13161

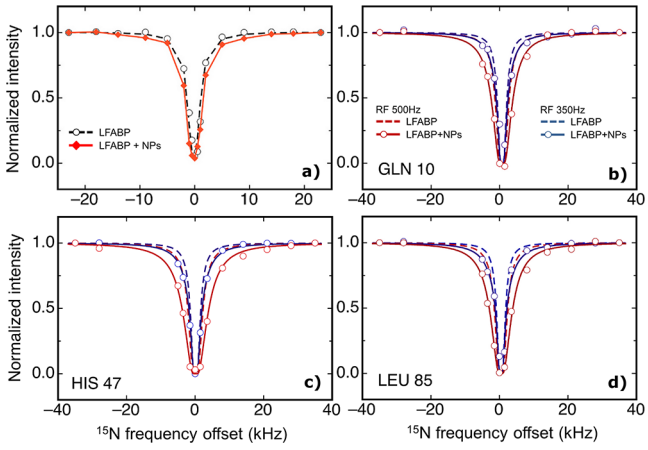


**Figure 2.** Dark-state effects on LFABP NMR signals. (a) Saturation profile of the 1D $H_N$ envelope of LFABP by transfer of $^{15}N$ saturation from the NP-bound state, measured at 14.1 T. (b–d) Representative residue-specific saturation profiles obtained with the 2D $^{15}N$-DEST experiment recorded at 23.5 T. Experimental data were collected on LFABP before and after addition of POPC:POPG–NPs in 50 mM KCl (protein:lipid molar ratio 1:40). The calculated best-fit curves are reported. Additional profiles are shown in Figure S6.

NPs, showing differences of up to 5 $s^{-1}$ (Figure S4). Differences in relaxation rates, $^{15}N$-$\Delta R_2$, may originate from chemical exchange line-broadening due to resonance frequency differences between the free and bound states, and/or to lifetime line-broadening due to large $R_2$ values in the bound state. The latter should be the dominant effect in the present case because $R_2$ were measured in a way that largely suppresses exchange-induced line-broadening and because we observed no correlation between $^{15}N$-$\Delta R_2$ values and $^{15}N$ exchange-induced shifts (Figure S5). In this regime, the maximum $^{15}N$-$\Delta R_2$ provides an estimate of the association rate constant $k_{on}^{app}$ for the pseudo-first-order process:

$$P + S \underset{k_{off}}{\overset{k_{on}^{app}}{\rightleftharpoons}} PS$$

where P is the free protein, S is the minimum binding unit on the NP surface (constituted by a number $n$ of lipids of the outer leaflet), PS is the unitary supramolecular adduct, $k_{off}$ is the first-order dissociation rate constant, and $k_{on}^{app} = k_{on}[S]$, $k_{on}$ being the second-order association rate constant. These relaxation data, together with the $k_{off}$ values estimated from real-time fluorescence, allowed us to obtain an estimate for the time scale of the exchange process, given by $\tau_{ex} = k_{ex}^{-1} = (k_{on}^{app} + k_{off})^{-1} \approx 190$ ms. The actual $\tau_{ex}$ value could be slightly underestimated due to a contribution to $^{15}N$-$\Delta R_2$ arising from the additional equilibrium of association between LFABP and single lipids extracted from the vesicles.

The above analyses are phenomenological and provide the important conclusion that NP-bound LFABP dynamics can be observed and that it is not homogeneous along the protein chain. A more quantitative analysis can be performed by simultaneous fitting of $^{15}N$-$\Delta R_2$ values and saturation profiles with the McConnell equations describing the relaxation of magnetization in the presence of chemical exchange.[18c] With the present system, the small observed $^{15}N$-$\Delta R_2$ and considerations on additional complexity deriving from competing equilibria with single phospholipid molecules prevented accurate deconvolution of $R_2$. We therefore attempted a quantitative analysis of DEST profiles only. 2D $^{15}N$-DEST data acquired in duplicate at 23.5 T static magnetic field using a saturation power level of 500 Hz reported significant saturation transfer and were fit using a simple two-state exchange model with a global kinetic adjustable parameter $k_{on}^{app}$ as well as site-specific $^{15}N$-$R_2^{bound}$ values. Reliable data could be obtained for 49 out of 127 amino acid residues distributed over the entire protein. The fitting resulted in estimated values of $k_{on}^{app} = 1.91 \pm 0.17$ $s^{-1}$ and $^{15}N$-$R_2^{bound}$ values as plotted in Figure 3.

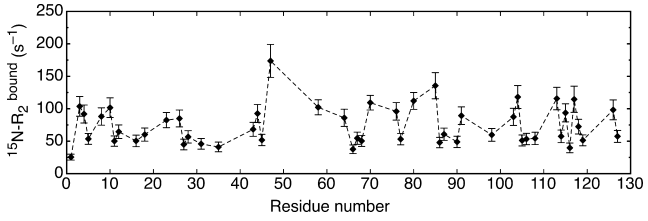


**Figure 3.** Residue-specific transverse relaxation rates of NP-bound LFABP determined by fitting DEST data.

Unexpectedly, the majority of the residues displayed $^{15}N$-$R_2^{bound}$ values around 50 $s^{-1}$, with peaks reaching 170 $s^{-1}$. If LFABP was tumbling with a rotational correlation time similar to that of a 100 nm hard particle (predicted to be about $7 \times 10^{-6}$ s), much larger $R_2$ values would be expected (above $10^4$ $s^{-1}$). It follows that NP-bound LFABP retains significant rotational dynamics. Still, a number of residues display considerably larger rates. By mapping the data on the protein structure, it can be observed that the residues with larger $^{15}N$-$R_2^{bound}$ are mostly located to the region opposed to the helix-turn-helix motif, called the anti-portal region (Figure 4).

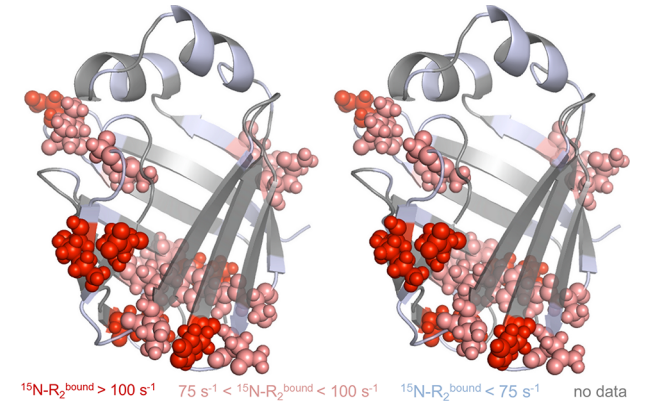


**Figure 4.** Mapping of residue-specific $^{15}N$-$R_2^{bound}$ values on the structure of LFABP (stereoview).

The partition depth of LFABP into NPs is not known; however, based on its known cytosolic distribution, as well as on fluorescence spectroscopy experiments on a closely homologous protein,[26] it can be inferred that the protein does not penetrate deeply into a lipid bilayer. It is then possible that LFABP offers a small interaction epitope and swivels around it with relatively unrestricted motion. Indeed, although rotational tumbling of peripheral proteins on the surface of lipid layers is poorly explored, it is known that a small penetration depth results in a reduced viscous drag, such that anchored proteins may display the same lateral diffusion rate as the lipid molecules themselves (about $10^{-8}$ $cm^2$ $s^{-1}$).[27] According to a previously proposed phospholipid anchorage model,[28] an extended lipid conformation could enable one aliphatic chain


dx.doi.org/10.1021/ja507310m | J. Am. Chem. Soc. 2014, 136, 13158–13161

to enter the protein cavity and act as a flexible protein anchor. A mechanism of phospholipid anchorage has also been proposed for cytochrome c and heat shock protein 70 binding to lipid membranes.[29,30] In the case of FABP the lipid cargo has been traditionally proposed to enter from the portal region formed by the helix-turn-helix motif and adjacent loops, but recent evidence point to alternative ligand exchange routes within the anti-portal region.[31] The possibility that the extended phospholipid chain interacts with this last epitope appears consistent with the larger $R_2^{bound}$ values observed with DEST. Increased values compared to the remainder of the protein could be ascribed to locally restricted motion and/or conformational exchange in the bound state around the lipid anchoring domain.

The DEST approach proved a powerful method to detect bound-state dynamics of a protein interacting with a soft NP without suffering from potential perturbations due to binding of free lipid molecules released from the NP. It can be predicted that the same advantage will apply to surfactant-stabilized NPs, because DEST will selectively report on interactions with the NP, not with the free surfactant molecules. More pronounced DEST effects are expected in cases where proteins retain fewer degrees of freedom in the NP-bound state. We believe that the approach proposed here constitutes a fundamental new tool for a deeper understanding of reversible protein−NP association equilibria.

## ■ ASSOCIATED CONTENT

### Supporting Information

Experimental procedures and six figures. This material is available free of charge via the Internet at http://pubs.acs.org.

## ■ AUTHOR INFORMATION


### Corresponding Author

michael.assfalg@univr.it


### Notes

The authors declare no competing financial interest.

## ■ ACKNOWLEDGMENTS

The work was supported by Cariverona Foundation (Nanomedicine Initiative Project). The authors are grateful for access to the 1 GHz NMR spectrometer at the NMR Facility in Lyon, provided under the 7th Framework Programme of the EC (Project No. 261863, Bio-NMR). We thank Dr. Daniele Dell'Orco for performing CD measurements and Dr. Clara Smal for help with fluorescence spectroscopy experiments.

## ■ REFERENCES


(1) Lynch, I.; Dawson, K. A. *Nano Today* **2008**, *3*, 40.
(2) Nicolini, C.; Bezerra, T.; Pechkova, E. *Nanomedicine* **2012**, *7*, 1117.
(3) Gagner, J. E.; Shrivastava, S.; Qian, X.; Dordick, J. S.; Siegel, R. W. *J. Phys. Chem. Lett.* **2012**, *3*, 3149.
(4) Monopoli, M. P.; Aberg, C.; Salvati, A.; Dawson, K. A. *Nat. Nanotechnol.* **2012**, *7*, 779.
(5) Sarikaya, M.; Tamerler, C.; Jen, A. K.-Y.; Schulten, K.; Baneyx, F. *Nat. Mater.* **2003**, *2*, 577.
(6) Texter, J.; Tirrell, M. *AIChE J.* **2001**, *47*, 1706.
(7) Mahmoudi, M.; Kalhor, H. R.; Laurent, S.; Lynch, I. *Nanoscale* **2013**, *5*, 2570.
(8) Linse, S.; Cabaleiro-Lago, C.; Xue, W.-F.; Lynch, I.; Lindman, S.; Thulin, E.; Radford, S. E.; Dawson, K. A. *Proc. Natl. Acad. Sci. U.S.A.* **2007**, *104*, 8691.
(9) Shemetov, A. A.; Nabiev, I.; Sukhanova, A. *ACS Nano* **2012**, *6*, 4585.
(10) Lundqvist, M.; Stigler, J.; Elia, G.; Lynch, I.; Cedervall, T.; Dawson, K. A. *Proc. Natl. Acad. Sci. U.S.A.* **2008**, *105*, 14265.
(11) Saptarshi, S. R.; Duschl, A.; Lopata, A. L. *J. Nanobiotechnol.* **2013**, *11*, 26.
(12) Eisenmesser, E. Z.; Bosco, D. A.; Akke, M.; Kern, D. *Science* **2002**, *295*, 1520.
(13) Wand, A. J. *Nat. Struct. Biol.* **2001**, *8*, 926.
(14) Dyson, H. J.; Wright, P. E. *Nat. Rev. Mol. Cell Biol.* **2005**, *6*, 197.
(15) Todorova, N.; Makarucha, A. J.; Hine, N. D. M.; Mostofi, A. A.; Yarovsky, I. *PLoS Comput. Biol.* **2013**, *9*, No. e1003360.
(16) Stueker, O.; Ortega, V. A.; Goss, G. G.; Stepanova, M. *Small* **2014**, *10*, 2006.
(17) Kleckner, I. R.; Foster, M. P. *Biochim. Biophys. Acta* **2011**, *1814*, 942.
(18) (a) Fawzi, N. L.; Ying, J.; Torchia, D. A.; Clore, G. M. *J. Am. Chem. Soc.* **2010**, *132*, 9948. (b) Fawzi, N. L.; Ying, J.; Ghirlando, R.; Torchia, D. A.; Clore, G. M. *Nature* **2011**, *480*, 268. (c) Fawzi, N. L.; Ying, J.; Torchia, D. A.; Clore, G. M. *Nat. Protoc.* **2012**, *7*, 1523. (d) Libich, D. S.; Fawzi, N. L.; Ying, J.; Clore, G. M. *Proc. Natl. Acad. Sci. U.S.A.* **2013**, *110*, 11361.
(19) Litt, J.; Padala, C.; Asuri, P.; Vutukuru, S.; Athmakuri, K.; Kumar, S.; Dordick, J.; Kane, R. S. *J. Am. Chem. Soc.* **2009**, *131*, 7107.
(20) (a) Torchilin, V. P. *Nat. Rev. Drug Discovery* **2005**, *4*, 145. (b) Puri, A.; Loomis, K.; Smith, B.; Lee, J.-H.; Yavlovich, A.; Heldman, E.; Blumenthal, R. *Crit. Rev. Ther. Drug Carrier Syst.* **2009**, *26*, 523. (c) Zhao, G.; Rodriguez, L. B. *Int. J. Nanomed.* **2012**, 61.
(21) Glatz, J. F.; van der Vusse, G. J. *Prog. Lipid Res.* **1996**, *35*, 243.
(22) Storch, J.; Corsico, B. *Annu. Rev. Nutr.* **2008**, *28*, 73.
(23) Ceccon, A.; D'Onofrio, M.; Zanzoni, S.; Longo, D. L.; Aime, S.; Molinari, H.; Assfalg, M. *Proteins* **2013**, *81*, 1776.
(24) Favretto, F.; Assfalg, M.; Gallo, M.; Cicero, D. O.; D'Onofrio, M.; Molinari, H. *ChemBioChem* **2013**, *14*, 1807.
(25) Ragona, L.; Pagano, K.; Tomaselli, S.; Favretto, F.; Ceccon, A.; Zanzoni, S.; D'Onofrio, M.; Assfalg, M.; Molinari, H. *Biochim. Biophys. Acta* **2014**, *1844*, 1268.
(26) Galassi, V.; Nolan, V.; Villarreal, M. A.; Perduca, M.; Monaco, H. L.; Montich, G. G. *Biochem. Biophys. Res. Commun.* **2009**, *382*, 771.
(27) Ziemba, B. P.; Falke, J. J. *Chem. Phys. Lipids* **2013**, *172−173*, 67.
(28) Hagan, R. M.; Worner-Gibbs, J.; Wilton, D. C. *Biochem. J.* **2008**, *410*, 123.
(29) Tuominen, E. K. J.; Wallace, C. J. A.; Kinnunen, P. K. J. *J. Biol. Chem.* **2002**, *277*, 8822.
(30) Mahalka, A. K.; Kirkegaard, T.; Jukola, L. T. I.; Jäättelä, M.; Kinnunen, P. K. J. *Biochim. Biophys. Acta* **2014**, *1838*, 1344.
(31) Long, D.; Mu, Y.; Yang, D. *PloS One* **2009**, *4*, No. e6081.